

Active Stability Control of a High-Beta Self-Organized Compact Torus

T. Asai 1), Ts. Takahashi 1), H. Matsunaga 1), H. Itagaki 1), Y. Matsuzawa 1), Y. Hirano 1),
To. Takahashi 2), M. Inomoto 3), L.C. Steinhauer 4) and A. Hirose 5)

1) College of Science & Technology, Nihon University, Tokyo, Japan

2) Graduate School of Engineering, Gunma University, Kiryu, Gunma, Japan

3) Graduate School of Frontier Sciences, The University of Tokyo, Kashiwa, Chiba, Japan

4) Department of Aeronautics & Astronautics, University of Washington, Seattle, WA, USA

5) Plasma Physics Laboratory, University of Saskatchewan, Saskatoon, SK, Canada

E-mail contact of main author: asai.tomohiko@nihon-u.ac.jp

Abstract. A magnetized coaxial plasma gun (MCPG) has been proposed as an effective device for control of a high-beta self-organized compact torus of field-reversed configuration (FRC). The initial results demonstrate that the application of an MCPG suppresses the most prominent FRC instability of the centrifugally-driven interchange mode with toroidal mode number $n = 2$. This observation was made on the Nihon University Compact Torus Experiment (NUCTE), a flexible theta-pinch-based FRC facility. In this series of experiments, a MCPG generates a spheromak-like plasmoid which can then travel axially to merge with a pre-existing FRC. Since the MCPG is mounted on-axis and generates a significant helicity, it provides the FRC-relevant version of coaxial helicity injection (CHI) that has been applied in both spheromaks and spherical tokamaks. When CHI is applied, the onset of elliptical deformation of FRC cross-section is delayed until 45 – 50 μs from FRC formation compared to the onset time of 25 μs in the case without CHI. Besides delaying instability, MCPG application reduces the toroidal rotation frequency from 67 kHz to 41 kHz. Moreover, the flux decay time is extended from 57 to 67 μs . These changes have been made despite the quite modest flux content of the plasmoid: ~ 0.05 mWb of poloidal and 0.01 mWb of toroidal flux, compared with the 0.4m Wb of poloidal flux in the pre-formed FRC. The observed global stabilization and confinement improvements suggest that the MCPG can actively control the rotational instability. This global instability can also be suppressed by externally applied static multipole fields. However, it has been known that nonaxisymmetric multipole fields have adverse effects on confinement. This indicates an advantage of MCPG in that it shows both improved confinement and stability. The conventional technique does not slow the toroidal rotation down. Therefore, the MCPG introduces a different stabilization mechanism that may be the same as that observed in translated FRCs [GUO, H.Y., et al., Phys. Rev. Lett. 95, (2005) 175001], i.e. because of an existence of modest toroidal flux.

1. Introduction

Use of a magnetized coaxial plasma gun (MCPG) has been proposed as an effective method of control for field-reversed configuration (FRC). Indeed, these initial results demonstrate the application of a MCPG suppresses the most prominent FRC instability. This observation was made on the Nihon University Compact Torus Experiment (NUCTE), a flexible θ -pinch-based FRC facility [1].

Pursuit of the FRC as fusion reactor core is motivated by highly favorable technological features: very high β , a natural divertor, linear device geometry, and axial mobility allowing separation of start-up and confinement functions. However, significant questions remain about the physics of FRCs, principally the global stability, the lack of effective control methods, and a fusion-relevant current drive. The highest quality (temperature, density) FRCs, formed by θ -pinch, have lifetimes limited to a few hundred microseconds, and scalability to larger sizes with long confinement and global stability has not been established. The MCPG, which can generate and accelerate magnetized plasmoid, emerges as a control method with multiple channels: suppression of instability, current sustainment, enhancement of radial electric field, and maintenance of a favorable balance between toroidal and poloidal fluxes.

The most dangerous global instability in a FRC is the rotational instability, which is the centrifugally-driven interchange mode with toroidal mode number $n = 2$. By this instability, the poloidal cross section of the plasma column deforms elliptically and then plasma touches the discharge tube wall, limiting the configuration lifetime τ_{FRC} to about one particle loss time τ_{N} .

Externally applied static multipole fields can suppress this rotational instability [2]. However, it has been found that the toroidal asymmetry of the multipole field has a negative effect on the confinement. To reduce asymmetry, a helical multipole field, in which a closed magnetic surface might be formed in the vicinity of the FRC separatrix while preserving the natural divertor, was applied. The stability threshold of the applied magnetic field is more effective than that of the straight one [3]. The positive effect on confinement properties, however, has not been observed [4].

Regarding rotational instability, the Translation Confinement Sustainment (TCS) facility had yielded promising results [5]. These results demonstrated suppression of the rotational mode as well as self-organization (conversion of toroidal to poloidal flux). Interpretive modeling of these observations also showed that the core of the FRC was a two-fluid minimum energy state [6], another marker of self-organization. This raised a new intriguing possibility that the modest toroidal field in these self-organized states may be the key to suppressing the rotational instability [7].

In this work, toroidal flux is actively injected into the FRC through the magnetized plasmoid formed by a MCPG. After a merging and relaxation process, FRC reaches the static equilibrium phase with a finite amount of magnetic helicity. The global stability of this FRC which toroidal flux is injected, is investigated experimentally.

2. Experimental Setup

2.1. Theta-pinch based FRC device

A series of experiments has been performed on the theta-pinch based FRC device, NUCTE-III [1]. A schematic diagram of the device is shown in Fig. 1. The central part of the theta pinch coil is 0.9 m in length and 0.34 m in inner diameter. A passive mirror coil of axial length 0.3 m and 0.32 m inner diameter is mounted at each end. These coils provide an on-axis vacuum mirror ratio of 1.13. The theta pinch coil is connected to a 5 kV, 1.92 mF slow capacitor bank,

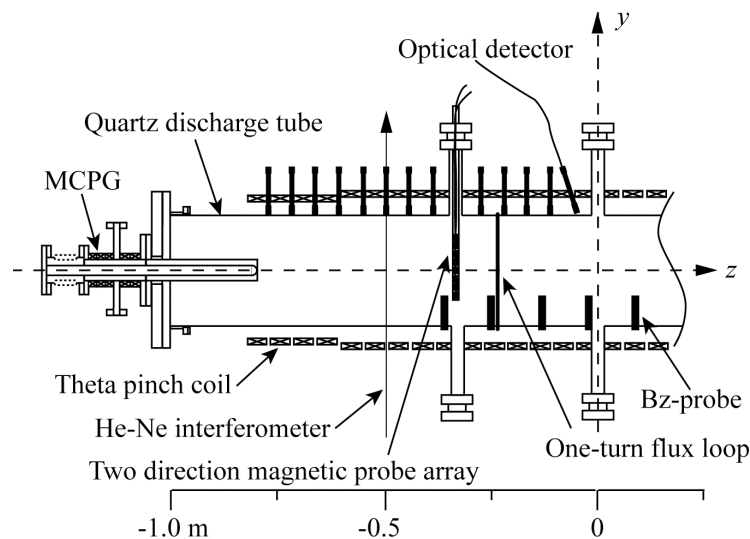


FIG. 1. Schematic view of NUCTE-III with a magnetized coaxial plasma gun.

a 25 kV, a 11.25 μF and a 32 kV, 67.5 μF fast capacitor bank. A transparent synthetic silica tube, 2 m in length and 0.256 m in diameter, is employed as a discharge chamber.

NUCTE-III is evacuated to 1.0×10^{-6} Torr and deuterium gas is filled into the discharge chamber. In the standard operation condition, the amount of filled gas is 10 mTorr. In this series of tests, preionization plasma is formed by the theta-discharge method. Then, a FRC plasma with separatrix radius of 0.05 m, length of ~ 1.3 m, and peak electron density of $\sim 2.5 \times 10^{21} \text{ m}^{-3}$ is generated.

The diagnostics for measuring typical plasma parameters consist of a helium-neon interferometer to measure line-integrated electron density $\int n_e dl$ and a flux loop with a set of magnetic probes to determine an axial profile of the separatrix radius $r_s(z)$ using the excluded flux method. Here, average electron density is estimated as $\int n_e dl / (2r_s)$. Typical plasma parameters are listed in Table I. The averaged number of ion gyro radii \bar{s} is the FRC's kinetic parameter, defined as $\bar{s} = \int_{R_0}^{r_s} (r/r_s \rho_i) dr = \Phi_p / (2\pi r_s B_e \rho_i)$. Here, R_0 is the field null axis, Φ_p the trapped poloidal flux inside the separatrix, ρ_i the ion gyro radii; and B_e the external magnetic field. Also, the proportion of \bar{s} relative to the FRC elongation E (\bar{s}/E) is listed for comparison with other devices. Here, E is defined as $E = l_s / 2r_s(0)$ (l_s : separatrix length).

Because of the transparent discharge chamber, the NUCTE device accepts optical diagnostics from all angles on the chamber surface. The optical diagnostic system consists of 60 collimators and each channel has a convex-plane lens (8mm in diameter, focal length $f = 100$ mm), glass optical fiber tubes, a band pass filter ($\lambda = 550 \pm 5$ nm for Bremsstrahlung and 655 ± 5 nm for Balmer- α) and a photomultiplier tube (PMT) [8]. In this series of tests, collimators have been placed in two arrangements. The first set of 21 collimators are azimuthally arranged at every 9° at the midplane of the translation region $z = -0.255$ m. The second set of 6 collimators are aligned parallel to the y-axis, spaced with intervals of 20 mm at $z = -0.270$ m. Each chord is parallel to the y-axis.

3.2. Magnetized Coaxial Plasma Gun

The MCPG consists of a formation and an acceleration region (Fig. 2). The formation region has an inner electrode and an outer electrode. A fast solenoid valve for deuterium gas puffing and a gun bias coil are mounted on the middle of the outer electrode. A gun bias field with a

TABLE I: Typical plasma parameters during standard operation

Plasma parameter	Standard operation
Filling pressure [mTorr]	10
Bias field [T]	0.032
Separatrix radius [m]	0.060
Separatrix length [m]	0.8
Electron density [$\times 10^{21} \text{ m}^{-3}$]	2.5
Total temperature [eV]	270
Particle confinement time [ms]	80
Number of ion gyro radii (\bar{s})	1.9
\bar{s}/E	0.28

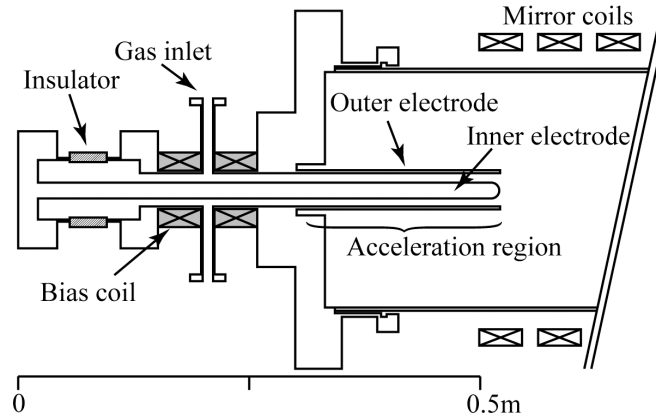


FIG. 2. Schematic view of the magnetized coaxial plasma gun.

flux of 0.074 mWb and a duration time of 200 μ s is driven by a 400 μ F capacitor with a charging voltage of 200 V. The electrodes are extended to the end of the theta-pinch coil and work as an accelerator. By the application of 22.5 kA of gun current with a pulse width of 15 μ s between the inner and outer electrodes and driven by a 20 kV-15 μ F capacitor, magnetized plasmoids are produced and rapidly accelerated.

Plasmoids with a velocity of about 40 km/s are injected into the vacuum vessel filled with a bias field of 0.032 T. The strength of the bias field also controls the process of plasmoid injection. A main reversed confinement field with a strength of 0.44 T, a 3 μ s rise time and a 120 μ s decay time are applied when the bias field strength rises to its maximum value. The discharge time sequence of these helicity injection experiments is shown in Fig. 3.

4. Experimental Results and Discussion

4.1. Magnetized Plasmoid

In this series of experiments, a magnetized plasmoid is injected into the vacuum vessel filled with 10 mTorr of deuterium gas. Figure 4 shows the typical magnetic structure of a plasmoid as measured by the two-directional internal magnetic probe array. The toroidal field is

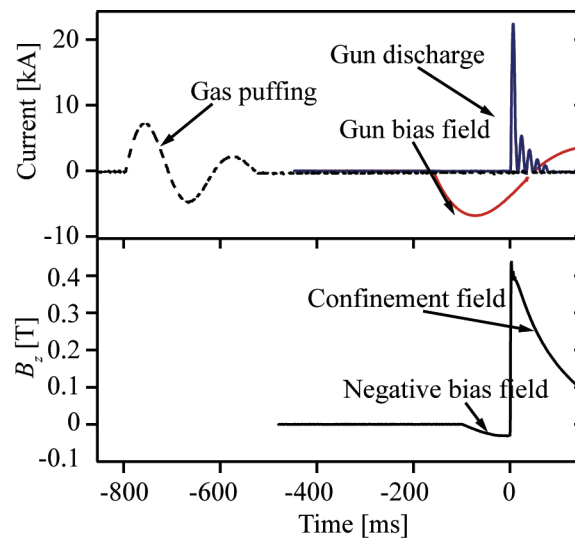


FIG. 3. Operation sequence of FRC formation and the MCPG.

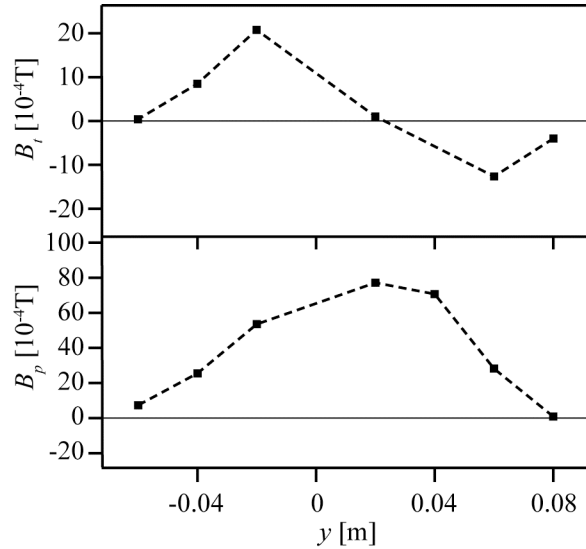


FIG. 4. Typical internal magnetic field profile of injected plasmoid.

reversed at about $y = 0.02$ m and the poloidal field has a peak at $y = 0.02$ m, confirming that a spheromak-like magnetic structure is produced by the MCPG. The separatrix radius and the length of the plasmoid are about 0.06 m and 0.40 m, respectively.

A spheromak-like plasmoid formed by the MCPG travels axially to merge with a pre-existing FRC, as was demonstrated on NUCTE. The arrangement of the MCPG and target FRC device, NUCTE is shown in Fig. 1, where the MCPG is mounted just beyond one end of the

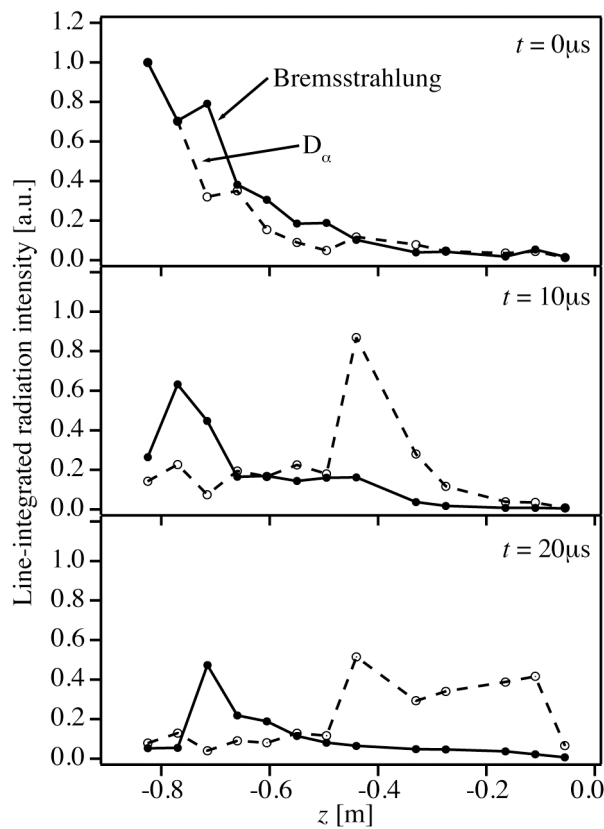


FIG. 5. Time evolution of axial emission profiles of the magnetized plasmoid. The solid line with closed circles indicates Bremsstrahlung and the dotted line and open circles Balmer- α .

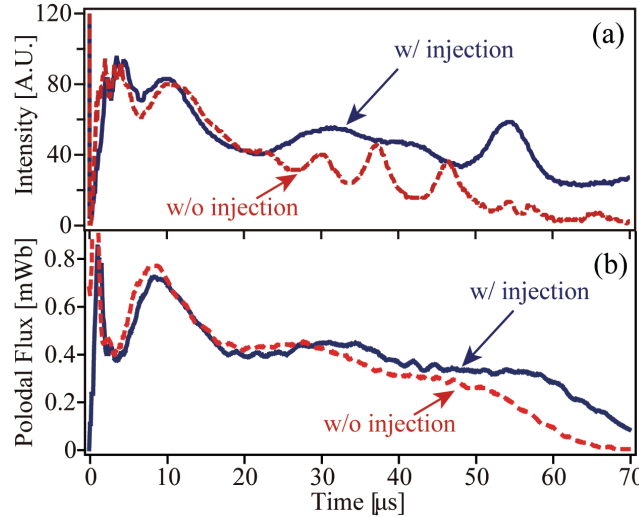


FIG.6. Time evolutions of (a) line-integrated Bremsstrahlung ($\lambda = 550 \pm 5\text{nm}$) and (b) poloidal flux.

mirror coil element. Since the MCPG is mounted on-axis and generates a significant helicity, it provides the FRC-relevant version of coaxial helicity injection (CHI) that has been quite successfully applied in both spheromaks and spherical tokamaks [9]. Once the plasmoid is generated by the MCPG, it extends axially and makes contact with the end of the FRC at about $25\ \mu\text{s}$ in this case. This creates a classic reconnection structure with anti-parallel “radial” fields at the contact surface. Rapid merging ensues, followed by self-organization within the merged object with a modest toroidal flux inherited from the plasmoid.

Figure 5 shows time evolution of the axial radiation profiles, which are emitted from the injected plasmoid traveling in the vacuum chamber filled with deuterium gas without FRC formation. The solid and the dotted lines are the line-integrated radiation intensity of Bremsstrahlung and the Balmer- α line spectrum, respectively. The strong emission of Balmer- α , which indicates plasma formation, appears at the front of the plasmoid. This indicates that the injected plasmoid ionizes filled neutral particles while penetrating into the vacuum vessel. The intensity of the Bremsstrahlung, which depends on the electron density, increases at the back side of the plasmoid. The plasmoid travels at $\sim 40\ \text{km/s}$ and is fully absorbed into the FRC after moving $\sim 0.5 - 0.6\ \text{m}$.

4.2. Stabilization of the rotational instability

The resulting toroidal field produces a dramatic effect on the rotational instability. Figure 6 (a) shows evidence for this on the bremsstrahlung emission I_b . The band range of $550 \pm 5\ \text{nm}$ is chosen to filter impurity line emission. Then, $I_b \propto n_e^2/\sqrt{T_e}$ [8], where n_e is electron density and T_e is electron temperature. Without CHI, oscillation on I_b rapidly sets in at about $25\ \mu\text{s}$, reflecting a rotating elliptical deformation of the FRC cross-section. When CHI is applied, the onset is delayed until $45 - 50\ \mu\text{s}$. The appearance of instability later may reflect the decay of the toroidal field. This might be delayed indefinitely by a more sustained or intermittent MCPG operation.

Besides delaying instability, MCPG application reduces the toroidal rotation frequency Ω_i from 4.2 to 2.6 [$10^5\ \text{rad/s}$]. Also, the e-folding time of flux τ_ϕ for the initial value in the equilibrium ($20\ \mu\text{s}$) is extended from 57 to $67\ \mu\text{s}$ (Fig.6 (b)). These achievements have been made despite the quite modest flux content of the plasmoid: $\sim 0.05\ \text{mWb}$ of poloidal and 0.01

mWb of toroidal flux, compared with the 0.4 mWb of poloidal flux in the pre-formed θ -pinch FRC.

5. Summary

The observed changes in the Bremsstrahlung and poloidal flux suggest that the MCPG can actively control the rotational instability. Improved confinement has also been shown. As mentioned above, this destructive instability can also be suppressed by externally applied static multipole fields [2-4]. However, it has been shown that nonaxisymmetric multipole fields have adverse effects on confinement [10]. This indicates an advantage of the MCPG in that it shows both improved confinement and stability. The conventional technique does not slow the toroidal rotation down. Therefore, the MCPG introduces a different stabilization mechanism that may be the same as observed in translated FRCs, i.e. because of a modest toroidal flux [5].

The MCPG also offers a number of other control channels. (1) Current drive, as in CHI on spheromaks and spherical tokamaks. (2) Plasma electrode: sustained plasmoid injection offers a control of the radial electric field, and thereby the edge rotational flow. (3) Refueling; plasmoid injection increases the plasma inventory. NUCTE is an ideal platform for investigating the MCPG as a multi-faceted control method in a broad range of parameters: density range of 1×10^{20} to $5 \times 10^{21} \text{ m}^{-3}$ and total temperature from 50 to 500 eV.

Acknowledgements

The support from Fusion Plasma Laboratory, Nihon University is gratefully acknowledged. This work was partially supported by Grant-in-Aid for Scientific Research (KAKENHI) 21740403 and 19560829, Nihon University Research Grant for 2009 and Nihon University Strategic Projects for Academic Research.

References

- [1] MATSUZAWA, Y., ASAI, T., TAKAHASHI, TS., et al., "Effects of background neutral particles on a field-reversed configuration plasma in the translation process", *Phys. Plasmas* 15, (2008) 082504.
- [2] OHI, S., MINATO, T., KAWAKAMI, Y., et al., "Quadrupole stabilization of the $n = 2$ rotational instability of a field-reversed theta-pinch plasma", *Phys. Rev. Lett.* 51, (1983) 1042.
- [3] SHIMAMURA S. and NOGI Y., "Helical quadrupole field stabilization of field-reversed configuration plasma", *Fusion Technol.* 9, (1986) 69.
- [4] REJ, D.J., ARMSTRONG, W.T., BARNES, G.A., et al., "Helical and straight quadrupole stabilization of the $n = 2$ rotational instability in translated field-reversed configurations", *Phys. Fluids* 29, (1986) 2648.
- [5] GUO, H.Y., HOFFMAN, A.L., STEINHAEUER, L.C., et al., "Observations of Improved Stability and Confinement in a High- β Self-Organized Spherical-Torus-Like Field-Reversed Configuration", *Phys. Rev. Lett.* 95, (2005) 175001.
- [6] STEINHAEUER, L.C. and GUO, H.Y., "Nearby-fluids equilibria. II. Zonal flows in a high-, self-organized plasma experiment", *Phys. Plasmas* 13, (2006) 052514.
- [7] MILROY, R.D. and STEINHAEUER, L.C., "Improved confinement and current drive of high temperature field reversed configurations in the new translation, confinement, and sustainment upgrade device", *Phys. Plasmas* 15, (2008) 056101.
- [8] TAKAHASHI, TS., GOTA, H., FUJINO, T., et al., "Multichannel optical diagnostic system for field-reversed configuration plasmas", *Rev. Sci. Instrum.* 75, (2004) 5205.

- [9] RAMAN, R., NELSON, B.A., BELL, M.G., et al., "Efficient Generation of Closed Magnetic Flux Surfaces in a Large Spherical Tokamak Using Coaxial Helicity Injection", *Phys. Rev. Lett.* 97, (2006) 175002.
- [10] OHKUMA, Y., TAKAHASHI, TS., SUZUKI, K., et al., "Effect of Multipole Fields on Field-Reversed-Configuration Plasma", *J. Phys. Soc. Japan* 63, (1994) 2845.